IEICE TRANS. COMMUN., VOL.E91–B, NO.6 JUNE 2008

PAPER Special Section on 2007 International Symposium on Antennas and Propagation

Performance Comparison of Detection Methods for Combined STBC and SM Systems

Xuan Nam TRAN[†a)], *Member*, **Huan Cong HO**[††], *Nonmember*, **Tadashi FUJINO**[††], *Member*, *and* **Yoshio KARASAWA**[††], *Fellow*

SUMMARY This paper considers detection schemes for the combined space-time block coding and spatial multiplexing (STBC-SM) transmission systems. We propose a symbol detection scheme which allows to extend the limit on the number of transmit antennas imposed by the previous group detection scheme. The proposed scheme allows to double multiplexing gain as well as provides better bit error rate (BER) performance over the group detection scheme. It is shown that the proposed QR-SIC (combined QR-decomposition and successive interference cancellation) symbol detector provides good trade-off between the BER and computational complexity performance and, thus, is the most suitable detector for the combined STBC-SM system.

key words: *transmit diversity, spatial division multiplexing, STBC, alamouti scheme*

1. Introduction

Recent researches on wireless communications have shown that multiple-transmit and multiple-receive antenna systems can increase channel capacity enormously in rich scattering fading environment [1], [2]. In order to achieve such promising capacity, two transmission techniques, known as space-time block coding (STBC) [3], [4] and spatial multiplexing (SM) [5], have been proposed to obtain either spatial diversity gain or spatial multiplexing gain, respectively. As each technique can achieve only either kind of the gains, it is natural to combine the two schemes to achieve both diversity and multiplexing gain at the same time [6], [7].

In the combined STBC-SM system, the transmit signal is first decomposed into G substreams corresponding to G groups of transmit antennas. Each substream is then space-time encoded and transmitted over its assigned group of transmit antennas. While merit of the combination is straightforwardly realized, the challenge lies in the detector used in the receiver due to the presence of interference among groups. In [7] Zhao and Dubey proposed a group detection scheme for combined STBC-SM systems using the Alamouti's STBC. The proposed scheme performs group detection to separate transmitted block codes from G groups first, then uses the Alamouti's space-time decoding algorithm to decode the signal encoded within each group. This group detection scheme is effective due to easy implementation with low complexity and provision of relatively good bit error rate (BER) performance. However, it suffers a lower limit $N \leq M$ on the number of transmit antennas, where N and M are the number of transmit and receive antennas, respectively. This means that for a MIMO system with M receive antennas, the maximum achievable multiplexing gain is limited to $M/2$. Another limitation of this scheme is that when zero-forcing (ZF) method is used to separate transmitted groups, matrix inversion of the channel matrix is not easily generalized for a system with a large number of antennas [7].

Recently, we have proposed a minimum mean square error (MMSE) detection scheme for a multiuser Alamouti's STBC system [8], [9]. Different from the group detection scheme, our scheme uses a simple processing scheme which allows to combine interference cancellation (IC) and space-time decoding together in a symbol detection manner. With M receive antennas, our detection scheme allows to support M users. As a multiuser STBC system and the combined STBC-SM system are equivalent, when applied to the STBC-SM system our symbol detection scheme allows to extend the lower limit on the number of transmit antennas from $N \leq M$ to $N \leq 2M$. This means that with the same number of receive antennas M, our proposed scheme can double the multiplexing gain of the combined STBC-SM system using the group-detection scheme. However, beside this advantage, it is still unclear whether the symbol detection scheme can also provide better BER performance (diversity gain) as well as whether it requires less complexity than the group detection scheme.

This paper aims to provide the answer for the above open question and to find out an efficient detector for the combined STBS-SM system. Our contributions include the following: (i) extensions of the MMSE symbol detector in [8], [9] to the case of ZF and the combined QR decomposition and successive interference cancellation (QR-SIC); (ii) detailed computational complexity analysis for both the group and symbol detection schemes using ZF, MMSE and QR-SIC method; and (iii) BER performance comparison of the two detection schemes for all three detection methods, namely, ZF, MMSE and QR-SIC using computer simulation. Our analysis shows that all ZF, MMSE, and QR-SIC symbol detectors outperform their corresponding group detectors in terms of BER performance. Although all symbol detectors require larger computational complexity than their

Manuscript received October 30, 2007.
Manuscript revised January 23, 2008.

[†]The author is with Le Qui Don Technical University, 100 Hoang Quoc Viet, Cau Giay, Hanoi, Vietnam.
[††]The authors are with The University of Electro-Communications, Chofu-shi, 182-8585 Japan.
a) E-mail: namtx@lqdtu.edu.vn

DOI: 10.1093/ietcom/e91–b.6.1734

corresponding group detectors, the QR-SIC symbol detector stands out to be the most suitable detector due to its good trade-off between the BER and computational complexity performance.

The remainder of the paper is organized as follows. Section 2 presents the system model for the combined STBC-SM system. The principles of the group and symbol detectors are presented in Sect. 3 and Sect. 4, respectively. Detailed complexity analysis is carried out in Sect. 5, followed by performance comparison in Sect. 6. Finally, conclusions are drawn in Sect. 7.

2. System Model

We consider a combined STBC-SM system in which the Alamouti's STBC [3] is used similar to that in [7]. Configuration of the system is illustrated in Fig. 1. We assume that N and M antennas are used in the transmitter and receiver, respectively. Different from [7], the correlation among receive antennas as well as among transmit antennas is assumed negligibly small so that we can ignore it for simplicity. Since the Alamouti's STBC is used the number of transmit antennas N is assumed to be an even number while the number of receiver antennas M can be any integer with an upper limit defined for each detection scheme presented in the following sections.

The channel between each pair of transmit and receive antennas is assumed to be independent and identically distributed (iid) with its complex gain modeled using a complex Gaussian variable with zero mean and unit variance. It is also assumed that the channel complex gain is constant within a block of symbols but varies from one to another. This assumption implies a quasi-static fading channel which facilitates the decoding algorithm for the Alamouti's STBC. The channel is also assumed to undergo flat fading so that channel equalization is not necessary at the receiver.

At the transmit side, a sequence of transmit symbols $\{s_k\}, k = 1, 2, \ldots, N$, is first divided into $G = N/2$ groups. The transmit vector to be sent over the 2 transmit antennas of the gth group is denoted as $\boldsymbol{s}_g = [s_{2g-1}, s_{2g}]^{\mathrm{T}}$, where the superscript $(\cdot)^{\mathrm{T}}$ denotes vector transposition. Similar to [7] it is assumed that the energy of the transmit symbols is normalized such that $E_s = \mathrm{tr}\{\mathrm{E}\{\|\boldsymbol{s}_g\|^2\}\} = 1$, where $\mathrm{E}\{\cdot\}$ and $\mathrm{tr}\{\cdot\}$ denotes the ensemble average operation and trace of a matrix, respectively. Each pair of two consecutive symbols s_{2g-1} and s_{2g} is then encoded using the Alamouti's STBC to generate a block code

$$\boldsymbol{S}_g = \begin{bmatrix} s_{2g-1} & -s_{2g}^* \\ s_{2g} & s_{2g-1}^* \end{bmatrix}, \tag{1}$$

where the superscript * denotes complex conjugation. Let us denote the complex gain of the channel from the first and second transmit antenna of the gth group to the mth receive antenna as $h_{m,2g-1}$ and $h_{m,2g}$, respectively. Since quasi-static fading is assumed the $M \times 2$ MIMO channel matrix corresponding to the channel from the gth group of transmit antennas to the M receive antennas is expressed as

$$\boldsymbol{H}_g = [\boldsymbol{h}_{2g-1}, \boldsymbol{h}_{2g}] \tag{2}$$

where

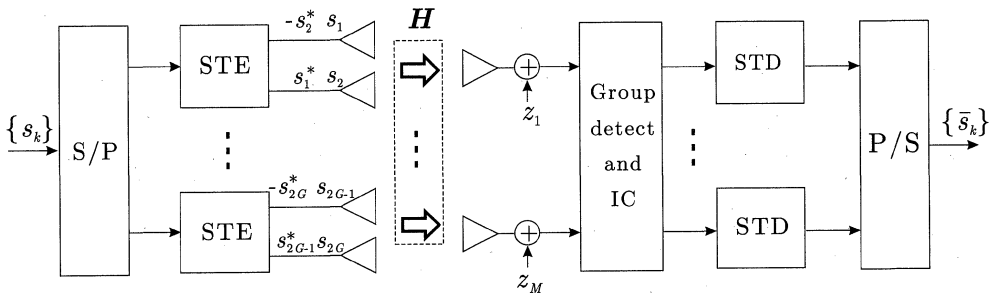

(a) Group detection receiver, $G=M/2$

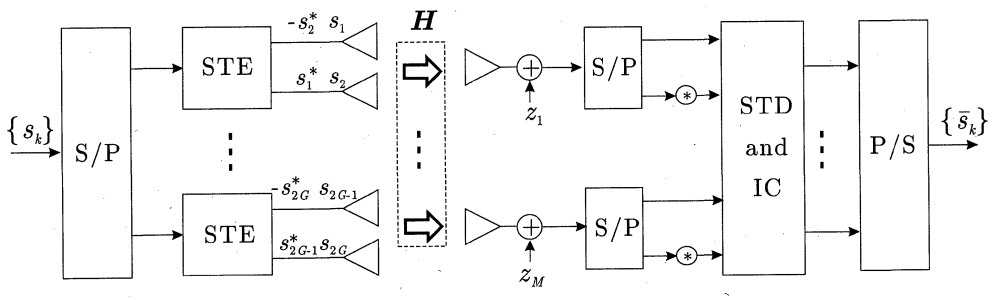

(b) Symbol detection receiver, $G=M$

Fig. 1 Configurations of detection methods for a combined STBC-SM system.

$$\boldsymbol{h}_{2g-1} = [h_{1,2g-1}, h_{2,2g-1}, \ldots, h_{M,2g-1}]^{\mathrm{T}} \quad (3)$$

$$\boldsymbol{h}_{2g} = [h_{1,2g}, h_{2,2g}, \ldots, h_{M,2g}]^{\mathrm{T}}. \quad (4)$$

The total channel matrix between the transmitter and receiver is then built by putting all G groups of the channel matrices together as

$$\boldsymbol{H} = [\boldsymbol{H}_1, \boldsymbol{H}_2, \ldots, \boldsymbol{H}_G]. \quad (5)$$

Arranging the transmit block code matrix $\boldsymbol{S}_g$ as

$$\boldsymbol{S} = [\boldsymbol{S}_1^{\mathrm{T}}, \boldsymbol{S}_2^{\mathrm{T}}, \ldots, \boldsymbol{S}_G^{\mathrm{T}}]^{\mathrm{T}}, \quad (6)$$

the receive matrix at two consecutive symbol time slots is given by

$$\begin{aligned} \boldsymbol{Y} &= \sum_{g=1}^{G} \boldsymbol{H}_g \boldsymbol{S}_g + \boldsymbol{Z} \\ &= \boldsymbol{H}\boldsymbol{S} + \boldsymbol{Z} \end{aligned} \quad (7)$$

where $\boldsymbol{Z} \in \mathbb{C}^{M\times 2}$ is the noise matrix containing iid complex Gaussian noise samples with power spectral density N_0.

3. Group Detection for Combined STBC-SM System

Based on the system model in (7), Zhao and Dubey proposed a group detection scheme which detects each transmitted block code $\boldsymbol{S}_g$, then uses the Alamouti's decoding algorithm to estimate single transmitted symbols s_{2g-1} and s_{2g}. The configuration of the group detection scheme is shown in Fig. 1(a). The principles of group detection based on ZF, MMSE, and QR-SIC are summarized below. For brevity, the Alamouti's decoding algorithm is omitted.

3.1 ZF Group Detection

The ZF group detector detects a desired block code by trying to remove interference from other block codes completely. Specifically, it uses a linear combining weight matrix $\boldsymbol{W}$ to make the channel matrix block diagonal as [7]

$$\boldsymbol{W}^{\mathrm{ZF}}\boldsymbol{H} = \mathrm{diag}\left\{\hat{\boldsymbol{H}}_1, \hat{\boldsymbol{H}}_2, \ldots, \hat{\boldsymbol{H}}_G\right\}. \quad (8)$$

where $\hat{\boldsymbol{H}}_g \in \mathbb{C}^{2\times 2}$ represents the virtual channel matrices corresponding to the gth block code. These virtual matrices are not unique and depend on the original channel matrix. For the case of a 4×4 MIMO channel matrix expressed as [7]

$$\boldsymbol{H} = \begin{bmatrix} \boldsymbol{H}_{11} & \boldsymbol{H}_{12} \\ \boldsymbol{H}_{21} & \boldsymbol{H}_{22} \end{bmatrix}, \quad (9)$$

with $\boldsymbol{H}_{ij} \in \mathbb{C}^{2\times 2}$, the linear combining weight matrix is given by

$$\boldsymbol{W}^{\mathrm{ZF}} = \begin{bmatrix} \boldsymbol{H}_{12}^{-1} & -\boldsymbol{H}_{22}^{-1} \\ \boldsymbol{H}_{11}^{-1} & -\boldsymbol{H}_{21}^{-1} \end{bmatrix}. \quad (10)$$

Thus the resulted block diagonal matrix becomes

$$\boldsymbol{W}^{\mathrm{ZF}}\boldsymbol{H} = \begin{bmatrix} \boldsymbol{H}_{12}^{-1}\boldsymbol{H}_{11} - \boldsymbol{H}_{22}^{-1}\boldsymbol{H}_{21} & \boldsymbol{0}_2 \\ \boldsymbol{0}_2 & \boldsymbol{H}_{11}^{-1}\boldsymbol{H}_{12} - \boldsymbol{H}_{21}^{-1}\boldsymbol{H}_{22} \end{bmatrix}.$$

where $\boldsymbol{0}_M$ represents an $M\times M$ matrix with all zero elements. Clearly, if we multiple $\boldsymbol{W}^{\mathrm{ZF}}$ in (10) with both sides of (7), the received matrix $\boldsymbol{Y}$ is decoupled into two separate groups as [7]

$$\tilde{\boldsymbol{Y}}_{2g-1} = \left(\boldsymbol{H}_{12}^{-1}\boldsymbol{H}_{11} - \boldsymbol{H}_{22}^{-1}\boldsymbol{H}_{21}\right)\boldsymbol{S}_{2g-1} + \tilde{\boldsymbol{Z}}_{2g-1} \quad (11)$$

$$\tilde{\boldsymbol{Y}}_{2g} = \left(\boldsymbol{H}_{11}^{-1}\boldsymbol{H}_{12} - \boldsymbol{H}_{21}^{-1}\boldsymbol{H}_{22}\right)\boldsymbol{S}_{2g} + \tilde{\boldsymbol{Z}}_{2g} \quad (12)$$

where $\tilde{\boldsymbol{Z}}_{2g-1} \in \mathbb{C}^{2\times 2}$ and $\tilde{\boldsymbol{Z}}_{2g} \in \mathbb{C}^{2\times 2}$ are the resulted noise matrices.

3.2 MMSE Group Detection

Using the MMSE method the linear combining weight matrix $\boldsymbol{W}_g$ used to detect the gth block code is the solution of the following cost function [7]

$$\begin{aligned} \boldsymbol{W}_g^{\mathrm{MMSE}} &= \arg\min_{\boldsymbol{W}_g} \mathrm{E}\left\{\left\|\boldsymbol{H}_g\boldsymbol{S}_g - \boldsymbol{W}_g\boldsymbol{Y}\right\|^2\right\} \\ &= \boldsymbol{H}_g\boldsymbol{H}_g^{\mathrm{H}}\left(\boldsymbol{H}\boldsymbol{H}^{\mathrm{H}} + N_0\boldsymbol{I}_M\right)^{-1} \end{aligned} \quad (13)$$

where $\boldsymbol{I}_M$ is an $M \times M$ identity matrix. The output corresponding to the gth group is given by [7]

$$\begin{aligned} \tilde{\boldsymbol{Y}}_g &= \boldsymbol{W}_g^{\mathrm{MMSE}}\boldsymbol{Y} \\ &= \boldsymbol{H}_g\boldsymbol{S}_g + \tilde{\boldsymbol{Z}}_g \end{aligned} \quad (14)$$

which contains only the desired block and resulted noise.

3.3 QR-SIC Group Detection

The QR-SIC group detector decomposes the channel matrix $\boldsymbol{H}$ into a unitary matrix $\boldsymbol{Q}$ and an upper diagonal matrix $\boldsymbol{R}$, i.e., $\boldsymbol{H} = \boldsymbol{Q}\boldsymbol{R}$. Then by multiplying both sides of (7) with $\boldsymbol{Q}^{\mathrm{H}}$, the output corresponding to the gth group is given by

$$\tilde{\boldsymbol{Y}}_g = \boldsymbol{R}_{g,g}\boldsymbol{S}_g + \sum_{i=g+1}^{G} \boldsymbol{R}_{g,i}\boldsymbol{S}_i + \tilde{\boldsymbol{Z}}_g \quad (15)$$

where $\boldsymbol{R}_{i,g} \in \mathbb{C}^{2\times 2}$ is a sub-matrix containing elements from rows $2i-1$ to $2i$ and from columns $2g-1$ to $2g$ of the upper triangular matrix $\boldsymbol{R}$. Note from (15) that the detection of the gth group only depends only on the lower groups, thus the QR-SIC group detector performs detection of the Gth group and decoding it first. Assume that $\boldsymbol{S}_G$ is correctly detected and decoded, then $\boldsymbol{S}_{G-1}$ can be obtained using (15). Similar operations are repeated for the remaining groups until all the transmitted block codes have been detected.

Having studied the principles of the above three group detectors, we can see that except the MMSE detector, both the ZF and QR-SIC group detector requires the number of receiver antennas M be not smaller than the number of transmitter antennas N. This constrain is necessary to ensure

proper solutions for the linear combining weight matrix $\boldsymbol{W}$ of the ZF detector and the QR decomposition of the QR-SIC detector. As a result, the number of transmit groups, and thus the multiplexing gain, is limited to $G = M/2$.

4. Symbol Detection for Combined STBC-SM Systems

In this section, we propose symbol detectors which allows to extend the limit on the number of transmitter antennas to $N \leq 2M$. This extended limit allows to double the multiplexing gain over the group detectors. The block diagram of the symbol detection scheme for the combined STBC-SM system is shown in Fig. 1(b).

We first convert the general signal model for the group detection scheme in (7) into a suitable model for the symbol detection scheme as in [8]. The idea is to combine and process the receive signal in two consecutive time slots at the same time. Based on Fig. 1, the received signal at each receiver antenna is first serial-to-parallel (S/P) converted into two branches so that the upper corresponding to the received signal at the first time slot and the lower the second. The lower branch is then complex-conjugated to rotate the phase of transmitted coded symbols at the second time slot. The inputs to the space-time decoder (STD) and interference canceller (IC) corresponding to the first and second time slot is given respectively by

$$\boldsymbol{y}_1 = [y_{1,1}, y_{2,1}, \ldots, y_{M,1}]^{\mathrm{T}} \tag{16}$$

$$\boldsymbol{y}_2^* = [y_{1,2}^*, y_{2,2}^*, \ldots, y_{M,2}^*]^{\mathrm{T}} \tag{17}$$

where $y_{m,t}, t \in \{1, 2\}$ represents the receive signals at the mth receive antenna at the first and second time slots, respectively. Arranging (16) and (17) we have

$$\boldsymbol{y} = [\boldsymbol{y}_1^{\mathrm{T}}, \boldsymbol{y}_2^{\mathrm{H}}]^{\mathrm{T}}. \tag{18}$$

Doing similarly for the noise components, we have

$$\boldsymbol{z}_1 = [z_{1,1}, z_{2,1}, \ldots, z_{M,1}]^{\mathrm{T}} \tag{19}$$

$$\boldsymbol{z}_2^* = [z_{1,2}^*, z_{2,2}^*, \ldots, z_{M,2}^*]^{\mathrm{T}} \tag{20}$$

and

$$\boldsymbol{z} = [\boldsymbol{z}_1^{\mathrm{T}}, \boldsymbol{z}_2^{\mathrm{H}}]^{\mathrm{T}}. \tag{21}$$

Due to this processing the transmit block code (1) reduces to simple a 2×1 vector

$$\boldsymbol{s}_g = [s_{2g-1}, \; s_{2g}]^{\mathrm{T}} \tag{22}$$

and the channel matrix $\boldsymbol{H}_g$ in (2) equivalently becomes

$$\bar{\boldsymbol{H}}_g = \begin{bmatrix} \boldsymbol{h}_{2g-1} & \boldsymbol{h}_{2g} \\ \boldsymbol{h}_{2g}^* & -\boldsymbol{h}_{2g-1}^* \end{bmatrix}. \tag{23}$$

Building the total transmit signal vector and channel matrix for all $G = M$ group as

$$\boldsymbol{s} = [\boldsymbol{s}_1^{\mathrm{T}}, \boldsymbol{s}_2^{\mathrm{T}}, \ldots, \boldsymbol{s}_G^{\mathrm{T}}]^{\mathrm{T}} \tag{24}$$

$$\bar{\boldsymbol{H}} = [\bar{\boldsymbol{H}}_1, \bar{\boldsymbol{H}}_2, \ldots, \bar{\boldsymbol{H}}_G] \tag{25}$$

we have the signal vector model used for symbol detection as follows

$$\boldsymbol{y} = \bar{\boldsymbol{H}}\boldsymbol{s} + \boldsymbol{z}. \tag{26}$$

Using this symbol detection model, both signal detection and space-time decoding are combined together. Since the number of rows of the channel matrix $\bar{\boldsymbol{H}}$ is doubled it is possible to extend the limit on the number of transmit antennas to $N \leq 2M$. Furthermore, the increase in the size of the receive signal $\boldsymbol{y}$ requires larger number of combining weights and thus better diversity gain is expected to obtain by the symbol detection scheme.

4.1 ZF Symbol Detection

Note that since the size of the channel matrix $\bar{\boldsymbol{H}}$ in (25) is $2M \times 2G$, the linear combining weight matrix of the ZF detector is

$$\bar{\boldsymbol{W}}^{\mathrm{ZF}} = \bar{\boldsymbol{H}}^{\dagger} \tag{27}$$

where the superscript † denotes the pseudo-inverse operation. The constrain on N such that ZF solution exists is thus $2G \leq 2M$ or $N \leq 2M$.

Using (27), the estimates of the transmitted vector $\boldsymbol{s}$ are given by

$$\bar{\boldsymbol{s}} = Q\{\bar{\boldsymbol{W}}^{\mathrm{ZF}}\boldsymbol{y}\} = Q\{\bar{\boldsymbol{H}}^{\dagger}\boldsymbol{y}\} \tag{28}$$

where $Q\{\cdot\}$ denotes the quantization function.

4.2 MMSE Symbol Detection

The solution of the linear combining matrix $\bar{\boldsymbol{W}}^{\mathrm{MMSE}}$ for the MMSE symbol detector given by

$$\bar{\boldsymbol{W}}^{\mathrm{MMSE}} = \arg\min_{\bar{\boldsymbol{W}}} \mathrm{E}\left\{\left\|\boldsymbol{s} - \bar{\boldsymbol{W}}\boldsymbol{y}\right\|^2\right\}, \tag{29}$$

$$= \bar{\boldsymbol{H}}^{\mathrm{H}}\left(\bar{\boldsymbol{H}}\bar{\boldsymbol{H}}^{\mathrm{H}} + N_0\boldsymbol{I}_{2M}\right)^{-1}. \tag{30}$$

The estimates of $\boldsymbol{s}$ is then given by $\bar{\boldsymbol{s}} = Q\{\bar{\boldsymbol{W}}^{\mathrm{MMSE}}\boldsymbol{y}\}$.

4.3 QR-SIC Symbol Detection

Similar to the QR-SIC group detector in Sect. 3.3, the QR-SIC symbol detector relies on QR decomposition of the channel matrix $\bar{\boldsymbol{H}} = \bar{\boldsymbol{Q}}\bar{\boldsymbol{R}}$ to obtain the upper triangular matrix $\bar{\boldsymbol{R}}$. Then by multiplying $\bar{\boldsymbol{Q}}^{\mathrm{T}}$ with both sides of (26) we can obtain the estimate s_k as

$$\hat{s}_k = r_{k,k}s_k + \sum_{i=k+1}^{N} r_{k,i}s_i + \tilde{z}_k, \tag{31}$$

where $r_{k,i}$ is the element at the kth row and ith column of $\bar{\boldsymbol{R}}$ and $\tilde{z}_k$ is the resulted noise components due to QR decomposition.

The QR-SIC detector then performs symbol detection

from symbol s_G to s_1 in a SIC manner. It is also noted that the constrain on the number of transmitter antennas N is $2M \geq 2G$ or $N \leq 2M$, which allows to double the multiplexing gain over the QR-SIC group detector.

5. Computational Complexity Analysis

In this section we perform a detailed complexity analysis of all the group and symbol detectors. The method of analysis follows that used in [9]. The complexity unit used in our analysis is the flop (FLoating-point OPeration) count. We would like to note that a complex multiplication $\mathbb{C} * \mathbb{C}$ requires 6 flops, a complex addition $(\mathbb{C} + \mathbb{C})$ 2 flops, a complex and real multiplication $\mathbb{C} * \mathbb{R}$ 2 flops, a complex and real addition $(\mathbb{C} + \mathbb{R})$ 1 flop, and finally both multiplication and addition of real numbers only 1 flop. It is also noted that in our analysis we take into account only the main sources of complexity such as computation of weight matrix, linear combining, QR decomposition and iterative detection, and the Alamouti's space-time decoding. Other minor complexity such as due to comparison, S/P conversion or complex conjugation is ignored for simplicity. In order to make the complexity representation simple, we set $N = M$ in our analysis. Furthermore, since the solution of the ZF detector in (10) cannot be directly generalized for an arbitrary M, we limit our analysis for the ZF group detector to the case of only a 4×4 MIMO system.

5.1 Complexity of ZF Detectors

5.1.1 Group ZF Detector

It is noted from (5) that for the case of group detection $\boldsymbol{H} \in \mathbb{C}^{M \times M}$ with $M = N$ then from (10), we have

$$C_{\boldsymbol{W}^{\mathrm{ZF}}} \sim \frac{M^3}{6}(\mathbb{C} * \mathbb{C}) + \frac{M^3}{6}(\mathbb{C} + \mathbb{C}) + \frac{M^2}{2}(\mathbb{C} * \mathbb{R}). \quad (32)$$

Since $\boldsymbol{Y} \in \mathbb{C}^{M \times 2}$, the combining operation of $\boldsymbol{W}^{\mathrm{ZF}}$ and $\boldsymbol{Y}$ requires

$$C_{\boldsymbol{W}^{\mathrm{ZF}}\boldsymbol{Y}} \sim 2M^2(\mathbb{C} * \mathbb{C}) + 2M^2(\mathbb{C} + \mathbb{C}) \quad (33)$$

From [3], we know that the complexity required to detect one block code is $4M(\mathbb{C} * \mathbb{C})$ and $6M(\mathbb{C} + \mathbb{C})$. Thus, the total complexity for decoding $G = M/2$ block code is

$$C_{\mathrm{gd}}^{\mathrm{STD}} \sim 2M^2(\mathbb{C} * \mathbb{C}) + 3M^2(\mathbb{C} + \mathbb{C}) \quad (34)$$

As a result, the total complexity required for the group detection ZF is summarized as

$$C_{\mathrm{ZF,gd}}^{\mathbb{C}*\mathbb{C}} = \frac{M^3}{6} + 4M^2 \quad (35)$$

$$C_{\mathrm{ZF,gd}}^{\mathbb{C}+\mathbb{C}} = \frac{M^3}{6} + 5M^2 \quad (36)$$

$$C_{\mathrm{ZF,gd}}^{\mathbb{C}*\mathbb{R}} = \frac{M^2}{2} \quad (37)$$

Converting to flops we have the total required complexity for the group detection ZF in flops given by

$$C_{\mathrm{ZF}}^{\mathrm{gd}} = \frac{4}{3}M^3 + 35M^2 \quad \text{[flops]} \quad (38)$$

5.1.2 Symbol-Detection ZF Detector

From (25) we have $\bar{\boldsymbol{H}} \in \mathbb{C}^{2M \times M}$, and thus the number of complex multiplications and additions required for calculating $\bar{\boldsymbol{W}}^{\mathrm{ZF}}$ are given by

$$C_{\bar{\boldsymbol{W}}^{\mathrm{ZF}}} \sim \left(\frac{13}{3}M^3 + 2M^2\right)(\mathbb{C} * \mathbb{C}) + \left(\frac{13}{3}M^3 + 2M^2\right)(\mathbb{C} + \mathbb{C}) \quad (39)$$

As $\boldsymbol{y} \in \mathbb{C}^{2M \times 1}$, the number of complex multiplications and additions required for multiplying $\bar{\boldsymbol{W}}^{\mathrm{ZF}}$ to $\boldsymbol{y}$ are given by

$$C_{\bar{\boldsymbol{W}}^{\mathrm{ZF}}\boldsymbol{y}} \sim \left(\frac{13}{3}M^3 + 2M^2\right)(\mathbb{C} * \mathbb{C}) + \left(\frac{13}{3}M^3 + 2M^2\right)(\mathbb{C} + \mathbb{C}) \quad (40)$$

In summary, the number of complex additions and multiplications required for the symbol-detection ZF detector are

$$C_{\mathrm{ZF,sd}}^{\mathbb{C}*\mathbb{C}} = \frac{13}{3}M^3 + 2M^2 \quad (41)$$

$$C_{\mathrm{ZF,sd}}^{\mathbb{C}+\mathbb{C}} = \frac{13}{3}M^3M^3 + 2M^2 \quad (42)$$

Converting to flops we have the total complexity of the symbol-detection ZF detector given by

$$C_{\mathrm{ZF}}^{\mathrm{sd}} = \frac{104}{3}M^3 + 16M^2 \quad \text{[flops]} \quad (43)$$

5.2 Complexity of MMSE Detectors

5.2.1 Group-Detection MMSE Detectors

Note from (13) the covariance matrix $\boldsymbol{R}_{xx}^{-1} = \left(\boldsymbol{H}\boldsymbol{H}^{\mathrm{H}} + N_0\boldsymbol{I}_M\right)^{-1}$ is common for all $G = M/2$ weight matrices $\boldsymbol{W}_g^{\mathrm{MMSE}}$. Complexity required for calculating $\boldsymbol{R}_{xx}^{-1}$ is

$$C_{\boldsymbol{R}_{xx}^{-1}} \sim \frac{4M^3}{3}(\mathbb{C}*\mathbb{C}) + \frac{4M^3}{3}(\mathbb{C}+\mathbb{C}) + M(\mathbb{C}+\mathbb{R}) + M(\mathbb{R}*\mathbb{R})$$

Converting this to flops we have

$$C_{\boldsymbol{R}_{xx}^{-1}} = \frac{32}{3}M^3 + 2M. \quad (44)$$

Furthermore, calculating $\boldsymbol{H}_g\boldsymbol{H}_g^{\mathrm{H}}$ requires $2M^2(\mathbb{C} * \mathbb{C}) + 2M^2(\mathbb{C}+\mathbb{C})$ and multiplying it to $\boldsymbol{R}_{xx}^{-1}$, $M^3(\mathbb{C}*\mathbb{C}) + M^3(\mathbb{C}+\mathbb{C})$. Converting both the complexities to flops gives $8M^3 + 16M^2$.

Thus the complexity for calculating $G = M/2$ weight matrices $\boldsymbol{W}_g^{\text{MMSE}}$ is

$$C_{\Sigma W_g} = \frac{32}{3}M^3 + 2M + \frac{M}{2}(8M^3 + 16M^2) \quad (45)$$

$$= 4M^4 + \frac{56}{3}M^3 + 2M \quad (46)$$

The complexity for combining $\boldsymbol{W}_g^{\text{MMSE}}\boldsymbol{y}$ requires $2M^2(\mathbb{C} * \mathbb{C}) + 2M^2(\mathbb{C} + \mathbb{C})$. As we need to do combining for all $M/2$ groups, the total complexity for combining is $\frac{M}{2}(16M^2) = 8M^3$. From (34) it is known that the complexity for space-time decoding $M/2$ groups is $18M^2$ flops.

In summary, the complexity of the group-detection MMSE detector is

$$C_{\text{MMSE}}^{\text{gd}} = 4M^4 + \frac{80}{3}M^3 + 18M^2 + 2M \text{ [flops]} \quad (47)$$

5.2.2 MMSE Symbol Detectors

Follow the analysis for the MMSE group detector above, we can have the complexity required for calculating the weight matrix $\boldsymbol{W}_{\text{MMSE}}^{\text{gd}}$ given by

$$C_{\boldsymbol{W}_{\text{MMSE}}^{\text{gd}}} \sim \frac{32}{3}M^3(\mathbb{C} * \mathbb{C}) + \frac{32}{3}M^3(\mathbb{C} + \mathbb{C}) + 2M(\mathbb{C} + \mathbb{R}) + 2M(\mathbb{R} * \mathbb{R}). \quad (48)$$

and the complexity combining $\boldsymbol{W}_{\text{MMSE}}^{\text{gd}}\boldsymbol{y}$ given by

$$C_{\boldsymbol{W}_{\text{MMSE}}^{\text{gd}}\boldsymbol{y}} \sim 2M^2(\mathbb{C} * \mathbb{C}) + 2M^2(\mathbb{C} + \mathbb{C}) \quad (49)$$

As a result, the total number of multiplications and additions needed for the MMSE group detector is

$$C_{\text{MMSE}}^{\text{sd}} \sim \left(\frac{32}{3}M^3 + 2M^2\right)(\mathbb{C} * \mathbb{C}) + \left(\frac{32}{3}M^3 + 2M^2\right)(\mathbb{C} + \mathbb{C}) + 2M(\mathbb{C} + \mathbb{R}) + 2M(\mathbb{R} * \mathbb{R}) \quad (50)$$

Converting to flops gives us the total complexity of the MMSE group detector as

$$C_{\text{MMSE}}^{\text{sd}} = \frac{256}{3}M^3 + 16M^2 + 4M \quad \text{[flops]} \quad (51)$$

5.3 Complexity of QR-SIC Detector

5.3.1 QR-SIC Group Detector

According to [10], the complexity required for decomposing $\boldsymbol{H} = \boldsymbol{QR}$ is

$$C_{\boldsymbol{QR}} \sim \left(M^3 + \frac{M^2}{2}\right)(\mathbb{C} * \mathbb{C}) + \left(M^3 + \frac{M^2}{2}\right)(\mathbb{C} + \mathbb{C}) + M^2(\mathbb{C} * \mathbb{R}) \quad (52)$$

Since $\boldsymbol{Q} \in \mathbb{C}^{M \times N}$ and $M = N$, we have the complexity for combining $\boldsymbol{Q}^H\boldsymbol{Y}$

$$C_{\boldsymbol{Q}^H\boldsymbol{Y}} \sim 2M^2(\mathbb{C} * \mathbb{C}) + 2M^2(\mathbb{C} + \mathbb{C}) \quad (53)$$

Then detecting group g, $g = G-1, G-2, ..., 1$, based on the SIC algorithm requires

$$C_{\text{SIC},g}^{\text{gd}} \sim 8(G-g)[(\mathbb{C}*\mathbb{C})+(\mathbb{C}+\mathbb{C})]+2(G-g)(\mathbb{C}+\mathbb{C}). \quad (54)$$

As we need to cancelation for group $G-1$ to 1, the complexity for detecting all G group using the SIC algorithm is

$$C_{\text{SIC}}^{\text{gd}} \sim \frac{8G(G-1)}{2}[(\mathbb{C}*\mathbb{C})+(\mathbb{C}+\mathbb{C})]+\frac{2G(G-1)}{2}(\mathbb{C}+\mathbb{C}) \quad (55)$$

Note that $G = M/2$ and take $C_{\boldsymbol{QR}}$ and $C_{\boldsymbol{Q}^H\boldsymbol{Y}}$ for calculation we have the complexity for QR-SIC given by

$$C_{\text{QR+SIC}}^{\text{gd}} \sim \left(M^3 + \frac{7}{2}M^2 - 2M\right)(\mathbb{C} * \mathbb{C}) + \left(M^3 + \frac{15}{4}M^2 - \frac{5}{2}M\right)(\mathbb{C} + \mathbb{C}) \quad (56)$$

Converting to flops we have

$$C_{\text{QR+SIC}}^{\text{gd}} = 8M^3 + \frac{57}{2}M^2 - 17M \quad \text{[flops]}. \quad (57)$$

Note from Sect. 5.2.1 that complexity for space-time decoding $G = M/2$ groups requires $18M^2$ flops, then the total complexity of the ZF-SIC group detector is given by

$$C_{\text{QR-SIC}}^{\text{gd}} = 8M^3 + \frac{93}{2}M^2 - 17M \quad \text{[flops]}. \quad (58)$$

5.3.2 QR-SIC Symbol Detector

Follow the analysis for the group QR-SIC detector, we can estimate the total complexity of the QR-SIC symbol detector as

$$C_{\text{QR-SIC}}^{\text{sd}} \sim \left(8M^3 + \frac{9}{2}M^2 - \frac{M}{2}\right)[(\mathbb{C} * \mathbb{C}) + (\mathbb{C} + \mathbb{C})] + 4M^2(\mathbb{C} + \mathbb{R}) \quad (59)$$

Converting to flops gives us

$$C_{\text{QR-SIC}}^{\text{sd}} = 64M^3 + 44M^2 - 2M \quad (60)$$

6. Performance Comparison Results

6.1 BER Performance Comparison

In order to obtain BER performance of the group and symbol detectors, we have carried out Monte Carlo simulations for the 4×4 and 4×2 combined STBC-SM systems using

QPSK modulation. For simplicity, both the channel matrix $\boldsymbol{H}$ and $\bar{\boldsymbol{H}}$ are assumed to be known at the receiver.

BER performance of all the detectors in the 4×4 combined STBC-SM system are compared in Fig. 2. The first observation can be made from the figure is that the proposed symbol detection scheme allows to achieve higher diversity order than the group detection one. This can be clearly seen in the figure by comparing the slope of BER curves obtained by the two schemes. The higher obtainable diversity order allows the proposed symbol detectors to achieve better BER performance than the group detectors. For example, at the same BER = 10^{-4} using the proposed symbol detection scheme, we can save up to about 3 dB in E_b/N_0 for the MMSE and QR-SIC detector. Larger improvement can be expected for the ZF detector. This higher diversity order and better BER performance improvement proves advantage of our proposed symbol scheme over the previously proposed group detection scheme of Zhao and Dubey in [7]. It is also seen that the MMSE and QR-SIC detector have almost the same BER performance while the ZF detector suffers BER degradation due to the noise amplification problem.

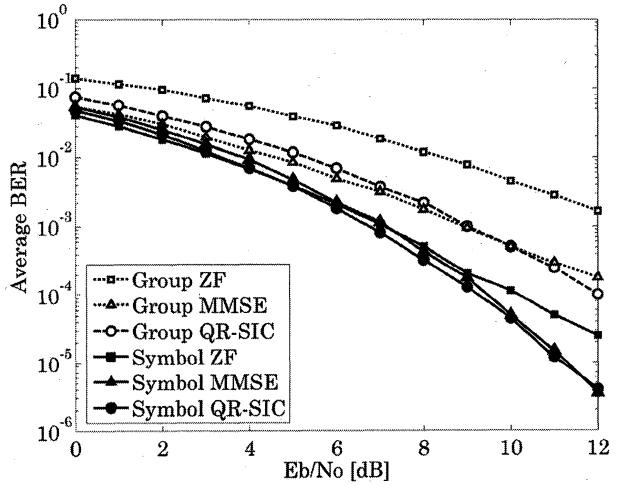

Fig. 2 BER performance in a 4×4 MIMO STBC-SM system.

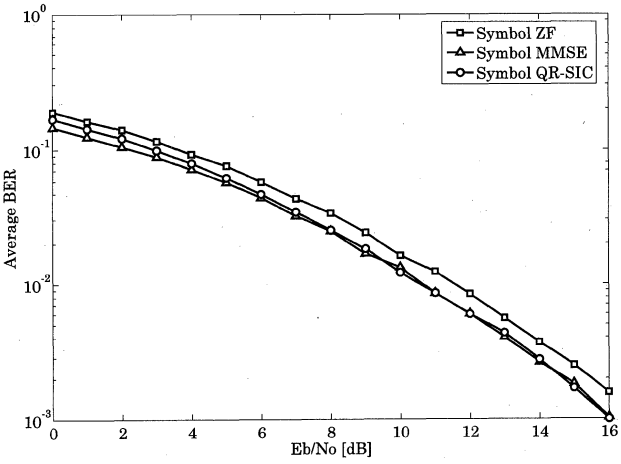

Fig. 3 BER performance in a 4×2 MIMO STBC-SM system.

Figure 3 shows the BER performance of the symbol detectors in a 4×2 STBC-SM system. From the results, it is clear that our proposed symbol detection scheme can be used for STBC-SM systems with $N \leq 2M$ with relatively good BER performance.

6.2 Computational Complexity Comparison

The estimated computational complexity for all the considered detectors is compared in Table 1. It can be seen that all the symbol detectors require much complexity than their corresponding group detectors. Particularly, for a 4×4 STBC-SM system, the ZF and QR-SIC symbol detectors requires up to about 4 times larger number of flops than their counterparts, respectively. For the MMSE detection, the symbol detector requires about twice the number of flops of the group one. This increase in computational complexity is due to the fact that the proposed symbol detection scheme processes the channel matrix with 2 times larger number of rows than the that with the group detectors.

It is also interesting to note that the difference ratio in computational complexity between the MMSE symbol detector and the group one reduces from about 2 times in a 2×2 MMIMO system to about 1.8 times in a 4×4 MIMO system. This is clear since the computational complexity order of the MMSE group detector is 4 while that of the symbol one is 3. As a result, the computational complexity of the MMSE symbol detector tends to become equivalent with that of the group detector in a combined STBC-SM system with larger number of antennas.

Combining both the BER and complexity analysis results, we can see that the QR-SIC symbol detector provides good trade-off between the two performance criteria, particularly as the number of antennas increases. Thus it is recommended to use the QR-SIC symbol detector for signal detection in the combined STBC-SM system.

7. Conclusions

In this paper we have proposed a symbol detection scheme

Table 1 Complexity comparison of the two detection schemes, $M = N$.

	ZF [FLOPS]	MMSE [FLOPS]	QR-SIC [FLOPS]
2×2 Group Detection	150	353	216
2×2 **Symbol Detection**	**341**	**750**	**684**
4×4 Group Detection	645	3,026	1,180
4×4 **Symbol Detection**	**2,474**	**5,733**	**4,792**

for the combined STBC-SM system and developed three detectors based on the ZF, MMSE, and QR-SIC methods. We have also carried out a detailed comparison between detectors based our proposed schemes with those based on the group detection scheme in terms of both BER and computational complexity performance. We have shown that the symbol detection scheme provides better BER performance and, more importantly, allows to extend the lower limit on the transmit antennas imposed by previous group detection scheme. Due to this extended limit, the symbol detection scheme allows to double the maximum multiplexing gain of the STBC-SM system. Finally, we have shown that among the considered detectors, the QR-SIC symbol detector seems to be most suitable for signal detection in the combined STBC-SM system due to its good trade-off between BER performance and associated computational complexity.

References

[1] G.J. Foschini and M.J. Gans, "On limits of wireless communications in a fading environment when using multiple antennas," Wirel. Pers. Commun., vol.6, pp.311–335, 1998.

[2] I.E. Telatar, "Capacity of multi-antenna Gaussian channels," European Trans. Telecommunications, vol.10, no.6, pp.585–595, Nov./Dec. 1999.

[3] S.M. Alamouti, "A simple transmit diversity technique for wireless communications," IEEE J. Sel. Areas Commun., vol.16, no.8, pp.1451–1458, Oct. 1998.

[4] V. Tarokh, H. Jafarkhani, and A.R. Calderbank, "Space-time block codes from orthogonal designs," IEEE Trans. Inf. Theory, vol.45, no.5, pp.1456–1467, July 1999.

[5] P.W. Wolniansky, G.J. Foschini, G.D. Golden, and R.A. Valenzuela, "V-BLAST: An architecture for realizing very high data rates over the rich-scattering wireless channel," Proc. URSI ISSSE'98, pp.295–300, Pisa, Italy, Sept. 1999.

[6] L. Zheng and D. Tse, "Diversity and multiplexing: A fundamental tradeoff in multiple antenna channels," IEEE Trans. Inf. Theory, vol.49, no.5, pp.1073–1096, May 2005.

[7] L. Zhao and V.K. Dubey "Detection schemes for space-time block code and spatial multiplexing combined system," IEEE Commun. Lett., vol.9, no.1, pp.49–51, Jan. 2005.

[8] X.N. Tran, T. Taniguchi, and Y. Karasawa, "Adaptive beamforming for multiuser space-time block coded systems," Proc. IEEE ISSSTA'04, pp.745–749, Sydney, Australia, Sept. 2004.

[9] X.N. Tran, T. Fujino, and Y. Karasawa, "An MMSE detector for multiuser space-time block coded OFDM," IEICE Trans. Commun., vol.E88-B, no.1, pp.141–149, Jan. 2005.

[10] G.H. Golub and C.F. Van Loan, Matrix Computation, 3rd ed., Johns Hopkins University Press, Baltimore, MD, 1996.

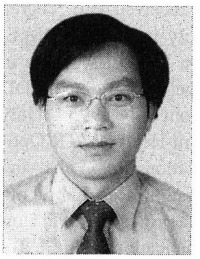

Xuan Nam Tran was born on the 8th September, 1971 in Thanh Hoa, Vietnam. He received his bachelor of engineering (BE) degree in radio-electronics from Hanoi University of Technology, Vietnam in 1993, master of engineering (ME) in telecommunications engineering from University of Technology Sydney, Australia in 1998, and doctor of engineering in electronic engineering from The University of Electro-Communications, Japan in 2003. From November 2003 to March 2006 he was a research associate at the Information and Communication Systems Group, Department of Information and Communication Engineering, The University of Electro-Communications, Tokyo, Japan. He is now with Faculty of Radio-Electronics, Le Qui Don Technical University, Hanoi, Vietnam. His research interests are in the areas of adaptive antennas, space-time processing, space-time coding and MIMO systems. Dr. Tran is a recipient of the 2003 IEEE AP-S Japan Chapter Young Engineer Award. He is a member of IEEE and Society of Information Theory and its Applications (SITA).

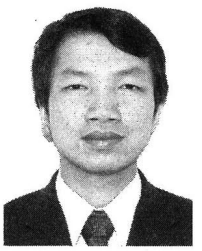

Huan Cong Ho was born in Vietnam in 1980. He received his bachelor of engineering in information and communication engineering in 2006 from The University of Electro-Communications, Tokyo, Japan. He is now with Mobile System Division, Global System Unit of Fujitsu Ltd., where he is working as an WiMAX Network Architecture Engineer

Tadashi Fujino was born in Osaka, Japan on 15 July, 1945. He received B.E. and M.E. degrees in electrical engineering and Ph.D. degree in communication engineering from Osaka University, Osaka, Japan, in 1968, 1970, and 1985, respectively. Since April 2000, he has been Professor in wireless communications at the Department of Information and Communication Engineering, The University of Electro-Communications, Tokyo, Japan. Before then, he had been with Mitsubishi Electric Corporation, Tokyo, Japan, since 1970, where he devoted in R&D in the wireless communications area such as digital satellite communications and digital land mobile communications. Currently, he is also a Visiting Professor at Bac Ha International University, Vietnam. His major works include the development of 120 Mbit/s QPSK modem and the trellis coded 8-PSK modem to operate at 120 Mbit/s for INTELSAT use, and portable phones PDC and PHS used in Japan and Asia and GSM used in Europe. He wrote a single authored book "Digital mobile communication," and four coauthored books. He holds over 20 patents. He received Meritorious Award from the ARIB (the Associate of Radio Industries and Businesses of Japan) of MPT of Japan, in 1997. Dr. Fujino is a Fellow of the IEEE. He is also a member of Society of Information Theory and its Applications.

Yoshio Karasawa received B.E. degree from Yamanashi University in 1973 and M.E. and Dr.Eng. Degrees from Kyoto University in 1977 and 1992, respectively. He joined KDD R&D Labs. in 1977. From July 1993 to July 1997, he was a Department Head of ATR Optical and Radio Communications Res. Labs. and ATR Adaptive Communications Res. Labs. both in Kyoto. Currently, he is a professor in the University of Electro-Communications (UEC), Tokyo, and a core member of Advanced Wireless Communication research Center (AWCC) in UEC. Since 1977, he has engaged in studies on wave propagation and antennas, particularly on theoretical analysis and measurements for wave-propagation phenomena, such as multipath fading in mobile radio systems, tropospheric and ionospheric scintillation, and rain attenuation. His recent interests are in frontier regions bridging "wave propagation" and "digital transmission characteristics" in wideband mobile radio systems such as MIMO. Dr. Karasawa received the Young Engineer Award from IECE of Japan in 1983 the Meritorious Award on Radio from the Association of Radio Industries and Businesses (ARIB, Japan) in 1998, Research Award from ICF in 2006, two Paper Awards from IEICE in 2006 and Best Tutorial Paper Award from Comm. Soc. of IEICE in 2007. He is a senior member of the IEEE and a member of SICE of Japan.